Modelling and simulation of short and long term membrane filtration experiments

Tomasz Janus*, Parneet Paul, Bogumil Ulanicki

Process Control – Water Software Systems, Department of Engineering, De Montfort University, Hawthorn Building, The Gateway, Leicester LE1 9BH, UK email: tjanus@dmu.ac.uk

ABSTRACT

Membrane bioreactors (MBRs) are a recent innovation in wastewater treatment that combines membrane filtration with biological processes [G. Tchobanoglous, F.L. Burton and H.D. Stensel, Wastewater Engineering, Treatment and Reuse, McGraw-Hill Professional, 2003, ISBN 0070418780, 9780070418783].The focus of this study is on membrane filtration. It concentrates on developing a mathematical model to describe filtration and fouling on micro and ultrafiltration membranes using work based on an earlier published model by Liang et al. (S. Liang, L. Song, G. Tao, K.A. Kekre and H. Seah, A modelling study of fouling development in membrane bioreactors for wastewater treatment, Water Environ. Res., 78(8) (2006) 857-863). Initial modelling experiments with Liang's model showed its deficiencies at predicting transmembrane pressures (TMPs) over a wide range of fluxes. A very basic structure of this model and its behavioural character limit its applicability to only a limited number of operational regimes. In an endeavour to develop a more universal yet simple model, the Liang model has been extended and modified to include: backwash mechanism; cake and soluble microbial product (SMP) deposit compressibility effects; various cake removal models (air scouring and crossflow velocity); and, flux dependent SMP deposition rates. The model was calibrated on experimental data from flux stepping experiments performed on a pilot scale membrane filtration unit with horizontal hollow fibres of 0.1 µm pore size and on a long-term filtration data from a MBR pilot plant equipped with vertical hollow fibres of similar pore size. The model proved to be in good agreement with the measurements in both calibration studies.

Keywords: Cake; Filtration; Fouling; MBR; Membrane; Modelling; Simulation; SMP; Wastewater

1. Introduction

1.1. Background

One of the main deficiencies of membrane bioreactors (MBRs) when compared to conventional wastewater treatment methods are larger operational costs due to higher energy consumption which is used for membrane backwashing, preventing cake build-up by air scouring or high crossflow velocities and for overcoming resistance of the membrane and foulants. The costs of chemicals used for regenerating the fouled membranes further add up to the operational expenses of MBRs. This research is focused at reducing these energy and chemical costs thereby making MBR systems more competitive as a treatment option. This can be achieved with improved system design, process optimisation and development of model

*Corresponding author

based control strategies based on validated mathematical models.

1.2. Mechanisms of membrane fouling

Membrane fouling in MBRs is attributed to the physicochemical interactions between the biofluid and the membrane [3]. Fouling is often subdivided into two subcategories: *reversible* fouling and *irreversible* fouling. Reversible fouling is caused by the deposition of suspended solids and formation of cake on the membrane surface. This cake layer build-up can be reduced by operation at low fluxes, and removed by backwashing, air sparging, provision of high crossflow velocities depending on the MBR configuration. Irreversible fouling is caused by constriction and blocking of membrane pores through adsorption of dissolved and some of colloidal matter. This type of fouling can only be removed by chemical cleaning. Restricting categorisation of membrane fouling to reversible and irreversible is however somewhat simplistic but is assumed so that mathematical models are in simpler form.

1.3. Factors affecting fouling

Fouling in MBRs is a very complicated process as it is induced by various types of foulants (i.e. solids, colloidal matter, and soluble substances) and caused by different mechanisms (i.e. cake and biofilm formation, adsorption, scaling, etc.). Findings of recent years show that fouling is influenced by the following factors: biomass characteristics [4] (e.g. floc size distribution and structure, extracellular polymeric substance (EPS) concentrations, and soluble microbial product (SMP) formation); plant configuration and operating conditions [5] (e.g. flux regime, periodical air or permeate backwash sequence, intermittent suction operation, air sparging intensity, crossflow velocity, solids retention time (SRT), mixed liquor suspended solids (MLSS) concentration, liquor viscosity, etc.); and membrane characteristics [6] (e.g. pore size distribution, membrane type, and material). For a given membrane type and fixed operating condition, fouling is then largely a function of SMP and EPS concentration and floc size distribution and interactions between floc size distribution and pore size distribution of the membrane. The exact relationships between these three factors and degree of fouling however are still unknown. As the floc size distribution of a polydisperse activated sludge is very difficult to determine, most research has focused on establishing correlations between fouling and EPS and SMP concentrations in the bulk liquid and the permeate. As the floc size distribution of an

activated sludge is very dependent on operational conditions [4] it is inevitable that floc and pore size distributions will have to be added to fouling models at some point. As reported in Nielsen and Jahn [7], the bound EPS in flocs is composed of sheaths, capsular polymers, condensed gel, loosely bound polymers and attached organic material. Unbound and therefore soluble EPS also known as SMP is composed of soluble macromolecules, colloids and slimes. The bound EPS and the SMP include bacterially produced polymers, and products of lysis and hydrolysis [8]. SMP is biodegradable and additionally can be a product of dissolution of bound EPS [9,10]. It is generally accepted that SMP contributes to irreversible fouling while suspended solids and bound EPS cause reversible fouling. EPS composition can affect some properties of activated sludge flocs and is reported to decrease the cake permeability [8,11]. Although the model described in this paper assumes the above mentioned relationships between fouling mechanisms and SMP and EPS, it is understood that connections between SMP, EPS and fouling are in fact much more complicated. It has been found [12] that not only concentrations of EPS and SMP but also the composition of SMP and EPS (i.e. the polysaccharide and protein content) have an effect of fouling properties of these components. Additionally SMP has been found to attribute not only to irreversible but also reversible fouling [12,13].

2. Modelling approaches to fouling

Capturing membrane fouling phenomena in the form of mathematical models has been a task of many different research groups around the world for more than a decade. The most common approach used is a resistance in series model which is given in Eqs. (1) and (2). In this approach, the total resistance of the membrane to liquid flow is equal to the sum of unit resistances such as pore constriction, cake, biofilm, polarisation layer, scaling, etc. Each model may have these separate phenomena modelled in a different way. Other aspects of MBR operation such as cake accumulation control with air sparging, crossflow velocity or backwashing will also need to be included in the MBR fouling model.

Since this fouling model is intended for MBR plant design, optimisation and model-based control applications, it needs to be simple enough to be calibrated with major biochemical and operational readings that are normally measured during daily plant operation. On the other hand it needs to describe the fouling phenomena with a sufficient level of detail in so it can be calibrated with a small number of parameters and for a

number of different MBR configuration encountered in practice. There are basically three main MBR configurations: (i) submerged hollow fibre which is backflushed and has coarse bubble air scouring; (ii) submerged flat plate which is non-backflushable but with coarse bubble air scour; and (iii) side stream crossflow which is not backflushed and usually has no air sparging as well.

2.1. Model selection and development – Liang's approach

As a base for model development the Liang model, the Liang model [2] was chosen as it has a simple mathematical structure which still proves relatively accurate during the calibration and validation studies. This model was then extended with additional mathematical equations so that it could accurately predict the TMPs under a range of operational conditions and for various different MBR configurations (e.g. submerged or sidestream crossflow). This model calculates TMP for a given flux using a resistance in series approach as described by Darcy in Eq. (1):

$$J = \frac{\Delta P}{\mu \cdot \sum R_i} = \frac{\Delta P}{\mu \cdot R_t} \tag{1}$$

where J is the permeate flux, m/s; ΔP is the TMP, Pa; μ is the dynamic viscosity of the permeate, Pa s; and R_t is the total resistance, 1/m.

Total resistance R_t is divided into three parts accordingly to the classical resistance in series model described in Eq. 2).

$$R_t = R_m + R_r + R_i \tag{2}$$

where R_m is the intrinsic membrane resistance, 1/m; R_r is the reversible (cake) resistance, 1/m; and R_i is the irreversible resistance caused by SMP deposit, 1/m.

The model represents two time-dependent resistances: resistance due to cake build-up (reversible fouling) and resistance due to SMP deposition on the membrane and inside the membrane pores (irreversible fouling). These resistances are proportional to the mass of cake and SMP deposited on the membrane and are given in Eqs. (3) and (4), respectively.

$$R_r = \alpha \cdot m_r \tag{3}$$

$$R_i = k_i \cdot m_i \tag{4}$$

where m_r is the mass of cake deposited on the membrane, kg/m²; m_i is the mass of SMP deposited on the membrane, kg/m²; α is the specific cake resistance, m/kg; and k_i is the fouling strength factor, m/kg.

Accumulation of m_r and m_i on the membrane is modelled with two ordinary differential Eqs. (5) and (6), respectively.

$$\frac{dm_r}{dt} = J \cdot X_T - k_r \cdot m_r \tag{5}$$

$$\frac{dm_i}{dt} = f_{SMP} \cdot J \cdot S_T \tag{6}$$

where X_T is the concentration of MLSS in the feed, g/m³; k_r is the cake detachment rate, 1/s; and S_T is the concentration of SMP in the feed, g/m³.

Originally the model assumed that all SMP in the feed ($f_{SMP} = 1$) is deposited inside the membrane pores or on top of the membrane and adds to the mass m_i. In fact the parameter f_{SMP} was not in the original Liang's model formulation and has been added by the authors to mathematically represent partial accumulation of SMP inside the membrane. The sludge cake is deposited on the membrane surface by the work of advection (i.e. mass flow of water through the membrane) but is also being detached by shear stresses caused by air scouring and crossflow velocity. The rate of cake removal is proportional to the mass of cake on the membrane. k_r is a function of many different operational parameters such as: membrane type, membrane chamber geometry, air sparging intensity, crossflow velocity, properties of the cake, etc. It can be linked to these and other operational variables using further mathematical formulae.

2.2. Extensions to the Liang's model

The following extensions were added to the original model equations.

2.2.1. Backwashing

The hollow fibres in a typical submerged MBR plant are backwashable, so this needed some representation in the model. The backwash sequence is modelled by resetting the initial conditions of differential Eqs. (5) and (6) after each backwash cycle. This means that after a backwash cycle has ended the mass of cake and deposited SMP can be reset to a defined value which is then used as the initial condition for the next forward filtration cycle as given in Eqs. (7) and (8).

$$m_r^{i+1}(t_F = 0) = fr_r \cdot m_r^i(t_F = t_{end}) \tag{7}$$

$$m_i^{i+1}(t_F = 0) = fr_i \cdot m_i^i(t_F = t_{end}) \tag{8}$$

where i is the filtration cycle number; t_F is the filtration cycle time, s; t_{end} is the filtration cycle duration, s; fr_f is the fraction of m_r remaining after the backwash (0–1); fr_i is the fraction of m_i remaining after the backwash (0–1).

Mass of cake and mass of SMP deposits at the beginning of the next forward filtration cycle is equal to a fraction of the mass of cake and SMP accumulated by the end of the previous filtration cycle. Forward filtration and backwash cycles are controlled in the model by a binary backwash logic signal where 0 stands for a forward filtration cycle and 1 for a backwash cycle.

2.2.2. Pressure dependency

In the original Liang formulation it is assumed that both cake and SMP deposits are incompressible while it has been reported that biological slurries are actually highly compressible [14]. Therefore compressibility Equations 9 and 10 for both the cake and the SMP have been added to the model. According to Flemming [15] as well as Lee and Wang [16], these are considered the most accurate equations for modelling cake compression and outperform several other simpler equations such as given in Parameshwaran et al. [17].

$$\alpha = \left(\frac{\Delta P}{\Delta P_{\text{crit}}^{\alpha}} + 1 \right)^{n_\alpha} \cdot \alpha_0 \tag{9}$$

$$k_i = \left(\frac{\Delta P}{\Delta P_{\text{crit}}^{k_i}} + 1 \right)^{n_{k_i}} \cdot k_{i0} \tag{10}$$

where $\triangle P_{\text{crit}}^{\alpha}$ is the threshold pressure below which no cake compression occurs, Pa; $\triangle P_{crit}^{ki}$ is the threshold pressure below which no compression of SMP deposits occurs, Pa; n_α is the cake compressibility factor; n_{ki} is the SMP deposit compressibility factor; α_0 is the specific cake resistance at atmospheric pressure, m/kg; and k_{i0} is the fouling strength factor at atmospheric pressure, m/kg.

The cake resistance according to Eq. (9) increases with TMP. For activated sludge the threshold pressure should be around 30 kPa [14]. The cake compressibility has reported values of $n = 0.8$–1.5. A realistic value of 1.0 was chosen for n_α and n_{ki} in this study. The parameter value of 1 produces a linear relationship between α, k_i and ΔP. The Liang's model with a backwash model and pressure dependency was calibrated to experimental data. During the calibration of the model with added compressibility effects and backwashing, it was found that the extended model was unable to predict TMP accurately at very low fluxes and was

therefore further modified in order to improve its accuracy over an entire operating region.

2.2.3. Flux dependent SMP deposition constant

In the research carried out by Ye et al. [18], the authors found that as the applied permeate flux decreases, the fraction of alginate protein deposited on the membrane pores gets smaller, with alginate used to model SMP. Ye's experiments showed an exponential relation between the permeate flux and SMP deposition rate which suggests a link between the deposition and the surface concentration as defined by the film model. Based on these research outcomes [18], Eq. (11) calculating fraction of SMP deposited on the membrane as an exponential function of flux has been developed.

$$f_{\text{SMP}} = \left|
\begin{array}{ll}
0 & \text{for} \quad J < J_{\min} \\
f_{\text{SMP,max}} \cdot (1 - \beta \cdot \exp -(J - J_{\min})) & \text{for} \quad J \geq J_{\min}
\end{array}
\right. \tag{11}$$

where $J_{\min}$ is the minimum flux below which no SMP deposition occurs, $1/(\text{m}^2 \text{ h})$; f_{SMP} is the fraction of SMP deposited on the membrane pores; $f_{\text{SMP,max}}$ is the maximum fraction of SMP deposited on the membrane pores; β is a constant determining how quickly f_{SMP} reaches $f_{\text{SMP,max}}$ with increasing flux.

2.2.4. Detachment rate with critical cake thickness

Detachment rate of the cake ($\dot{m}_r$) is most likely to be dependent on the cake thickness for a given air scouring intensity or crossflow velocity as thicker cakes are less bound to the membrane layer and therefore are easier to detach. The Liang's model assumes that cake detachment $\dot{m}_r$ is proportional to the mass of cake deposited on the membrane according to expression: $k_r \cdot m_r$ (as in Eq. (5)). This entails close to zero cake detachment rates at lower fluxes where cake deposition is low and leads to formation of thin cake layers at low fluxes. These thin cake deposits then create small TMP jumps in filtration cycles which are not observed in practice. Hence the modified model assumes a threshold cake thickness d_{crit} below which the mass flux of detached cake $\dot{m}_r$ is constant and equal to $\dot{m}_{r1}$. For thicker cake layers the detachment rate is a function of cake thickness as shown in Eq. (12).

$$\dot{m}_r = \left|
\begin{array}{ll}
\dot{m}_{r,1} & \text{for} \quad d < d_{\text{crit}} \\
\dot{m}_{r,1} + k_{r,2} \cdot (d - d_{\text{crit}}) & \text{for} \quad d \geq d_{\text{crit}}
\end{array}
\right. \tag{12}$$

where d is the cake thickness, m; d_{crit} is the critical cake thickness, m; $m_{r,1}$ is the detachment rate, kg/(m^2·d); and $k_{r,2}$ is the detachment parameter, kg/(m^3·d).

The cake thickness is calculated from the mass of cake according to Eq. (13).

$$d = f \cdot \frac{m_r}{\rho_c} \quad (13)$$

where m_r is the mass of cake per membrane area, kg/m^2; ρ_c is the wet cake density, kg/m^3; and f is the ratio of the wet weight to the dry weight of the sludge cake.

For activated sludge, the values of $\rho_c = 1.06 \times 10^3$ kg/m^3 and $f = 3.45$ have been previously determined by Li and Yuan [19]. To account for pressure compressibility effects, the wet cake density, ρ_c, should really be a function of pressure and not a constant value as used here for the sake of simplicity.

2.2.5. Shear stress model

Nagaoka et al. [20] presented a mathematical relationship between the cake detachment rate and shear stresses, τ_m, caused by crossflow velocity (and/or air bubbles from scouring). The detaching force due to τ_m is diminished by a pressure dependent static friction term which determines how strongly the cake adheres to the membrane. The expression for $k_{r,N}$ is presented in Eq. (14).

$$k_{r,N} = \gamma_m \cdot (\tau_m - \lambda_m \cdot \Delta P) \quad (14)$$

where $k_{r,N}$ is the Nagaoka's cake detachment rate, 1/s; γ_m is the constant, 1/Pa s; τ_m is the shear stress, Pa; and λ_m is the static friction coefficient, -.

The value of τ_m can be correlated with crossflow velocity and air scour intensity, which directly links a detachment rate parameter k_r to operational conditions in a MBR system.

Nagaoka's shear stress model was introduced into Eq. (13) by replacing the parameter $k_{r,2}$ with cake detachment value from Eq. (14). As $k_{r,N}$ denotes cake detachment per unit mass and $k_{r,2}$ is a detachment constant per unit cake thickness, conversion between these two parameters needs to be applied as shown in Eq. 15 below.

$$k_{r,2} = \frac{k_{r,N} \cdot \rho_c}{f} \quad (15)$$

In this way, the shear stress model can be introduced into the detachment model with critical cake thickness.

2.2.6. Back transport model

Ho and Zydney [21] introduced a back transport equation which determines the rate of cake removal due to hydrodynamic forces (i.e. inertial lift and shear induced diffusion) acting on the cake layer. Back transport rate, $\dot{M}_{det}$ is equivalent to the term $k_r \cdot m_r$ in Eq. (5). This model extension is described in Eq. (16).

$$\dot{M}_{det} = k \cdot \gamma^n \cdot \text{MLSS} \quad (16)$$

where $\dot{M}_{det}$ is the back transport rate, kg/m^2/s; k is the proportionality constant, m/(s^{1-n}); γ is the shear rate (crossflow velocity), 1/s; and n is a constant, $n = 1$ for shear induced diffusion, $n = 2$ for inertial lift.

The term $k \cdot \gamma^n$ refers to the steady state flux which increases with increasing particle radius, a, with a dependence of a^3 for inertial lift and $a^{1.33}$ for shear induced diffusion. Thus large cells and flocculated material tend to be kept away from the membrane surface with the steady state flux dominated by the smaller colloidal matter [21]. A number of investigators have developed empirical correlations for the steady state flux in terms of the wastewater properties and operating conditions [22,23]. However, the functional form and parameters are likely to be unique to the membrane, module design, wastewater, and biological condition of the activated sludge, so were not included in this generalised model.

3. Model calibration

3.1. Experimental procedures

The developed fouling model has been calibrated on two sets of data. The first, short-term filtration set has been obtained during flux stepping tests performed on an ITT Sanitaire pilot membrane filtration unit. The second, long-term set has been obtained from a pilot submerged MBR plant.

The first unit was a simple filtration cell fed with treated effluent coming from a sequencing batch reactor having low TSS (total suspended solids) and low COD which was mostly composed of SMP. Low suspended solids levels mean that multiple flux steps can be carried out in the unit in a single day, which speeds up the experimental procedure, without repeated clogging or even permanent membrane damage occurring. The concentration of TSS was however large enough to create cake buildup on the membrane surface during the filtration cycles as shown in Figs 1-4. Table 1 lists the unit s main operational data. In this flux stepping experiment the membrane was subjected to a range of fluxes from 30 l/(m^2 h) to 55 l/(m^2 h) in 5 l/(m^2 h)

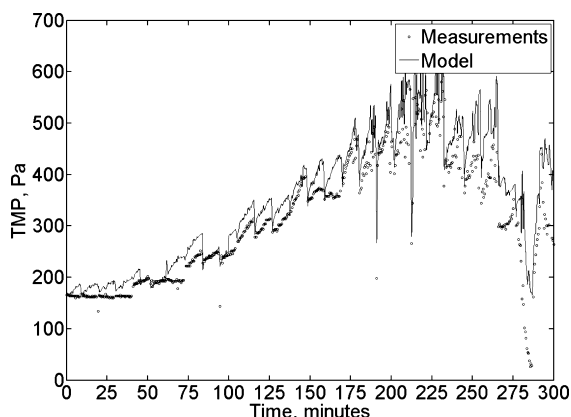Fig. 1. Simulation option 1 (as in Table 2).

Fig. 3. Simulation option 3 (as in Table 2).

increments. This allowed for testing the irreversible and reversible fouling under various fluxes both below and above the critical flux. Parameters of different submodel combinations constituting the fouling model were estimated using a combination of manual procedures and the Nelder-Mead optimisation algorithm. The objective function for optimisation-based calibration was a sum of absolute differences between measurements and the model output.

The second unit was a pilot submerged MBR plant equipped with a hollow fibre PES (polyethersulfone) membrane fed with brewery wastewater (see Table 4). Dimensions of the filtration portion of the pilot MBR unit were identical to the filtration unit used in the initial model calibration step. The long-term calibration was done on standard mixed liquor from a MBR plant to test the model predictability during filtration of liquids with high biological solids content. For this calibration exercise, filtration data for a 650 hour long period was used.
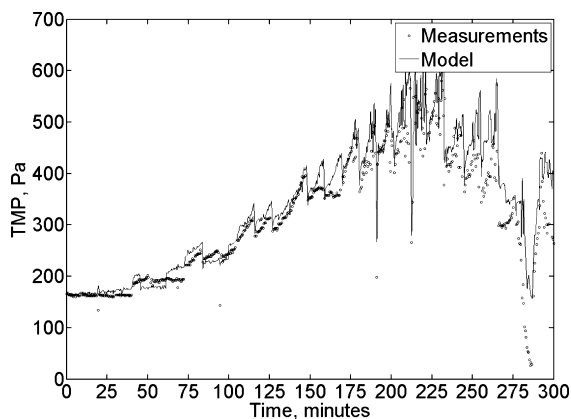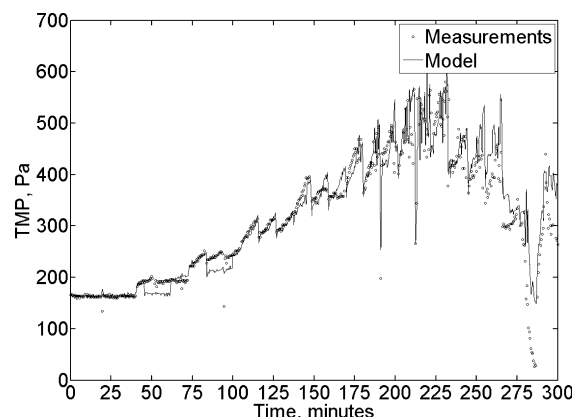
3.2. Calibration results – flux stepping

In order to calibrate the unknown parameters in each and every submodel, the calibration procedure was split into 4 separate tasks in which different parts of the model were simulated. The submodel combinations that were used are shown in Table 2. In the course of the following 4 calibration procedures all required unknown parameters have been estimated. Then each unique calibrated model has been simulated and results, as shown in Figs. 1–4, were compared against each other.

As shown in Fig. 1 Liang's model with compressibility effects and a backwash module showed some inabilities to predict the reversible and irreversible fouling especially at lower applied permeate fluxes. Hence at low fluxes, the model predicts cake deposition (i.e. reversible fouling) even at sub critical fluxes whereas the experimental data show no cake accumulation in this region. This is caused by the cake removal term $kr \cdot mr$ in Eq. (5) which tends to zero at low mr values and this then creates an opportunity for thin
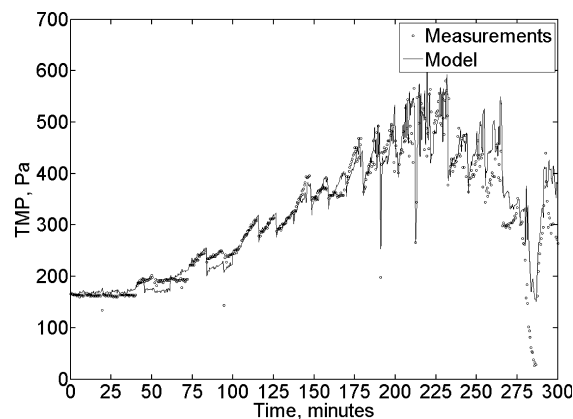

Fig. 2. Simulation option 2 (as in Table 2).

Fig. 4. Simulation option 4 (as in Table 2).

Table 1
Pilot membrane filtration unit operational data

Membrane filtration unit (without bioreactor)	
Membrane type and area	Horizontal ''Kolon'' fibres; PVDF 0.1 μm pore size; 20 m^2
Feed flow; permeate flow; backwash	1–2.4 m^3/h; 0.6–1 m^3/h; 1.2–1.8 m^3/h
Backwash interval and duration	Every 4 min with 30 s ON
TMP	300–500 mbar
Aeration rate	13 Nm^3/h from coarse bubble tube diffuser
Cleaning regime	Hypochlorite dosed 4 times daily into permeate tank
Biological feed data	COD $\sim$ 50 mgO$_2$/l; TSS $\sim$ 25 mg/L
SMP feed data	Glucose $\sim$ 5 mg/l; proteins $\sim$ 100 mg/L

layers of cake to build-up on the membrane surface. The longer term TMP build-up which can be manually calculated as the difference in the TMP between the start of each consecutive filtration cycle after a full backwash and under a constant flux is due to SMP accumulation (irreversible fouling). The experimental data show no long-term TMP gradient in the first 35 min of operation where the flux was kept at a constant value of $\sim$30 l/(m^2 h). This leads to a conclusion that SMP deposition at low fluxes is minimal. The long-term TMP gradient gets larger as the experiment progresses and as the applied flux gets higher. This leads to the conclusion that SMP deposition rate is a function of the applied flux. As the original Liang's model assumes a constant SMP deposition rate regardless of the applied flux, the SMP deposition constant is chosen for an entire range of fluxes. This results in non-zero irreversible fouling at even very small applied fluxes (Figs. 1 and 2).

In order to improve the model with regards to cake fouling at low fluxes, the cake detachment rate was modelled with Eqs. (12) and (13). Introduction of this new submodel added two new unknown parameters but improved the model performance under low flux conditions as well as at higher applied fluxes, i.e. between the 75th- and the 150th-min of operation. The long-term TMP gradient due to irreversible fouling is still present at low applied fluxes as shown in Fig. 2.

Outputs from the Liang's model with thickness dependent cake removal using the shear stress model as a replacement for the $k_{r,2}$ parameter and flux dependent SMP deposition are shown in Fig. 3. The model is able to represent the long-term and short-term TMP gradients quite accurately in an entire range of applied fluxes and throughout the duration of the experiment. The model begins to diverge from the experimental data at higher applied fluxes where TMP rises above 450 Pa. This divergence is not caused by the model formulation, but is rather due to fluctuations in pressure and flow meter readings taken on the permeate side of the membrane. These fluctuations are caused by cavitation effects and degassing of dissolved gases at large negative suction pressures. It is worth noting that the model diverges from the measurements in the down stepping part of the flux stepping experiment. It is supposed that this temporary divergence is caused by rapid pressure transients occurring in the membrane and permeate pipework which the model is not able to pick up. However, this model has been designed to predict operation of a membrane under normal operating conditions and thus accurate representation of TMP at large flux steps has never been our objective.

An alternative cake detachment model to the shear stress model, called a back transport model [21] which relates the detachment rate to shear stresses and solids concentration in the bulk liquid is simulated in Fig. 4. For this particular experiment the back transport model produced almost identical results to the cake detachment model with critical cake thickness using a parameter calculated with a shear stress model (Fig. 3).

All calibrated parameters are collated and presented in Table 3.

Table 2
Modified Liang model with various submodel combinations

Fig. 1 – option 1	Basic model with backwashing and compressibility effects, (A)
Fig. 2 – option 2	(A) With critical cake thickness detachment rate
Fig. 3 – option 3	(A) With critical cake thickness detachment rate, shear stress model, and flux dependent SMP deposition
Fig. 4 – option 4	(A) With back transport model and flux dependent SMP deposition rate

Table 3
Calibrated parameters of the multi-configurable fouling model

Parameter	Value	Unit	Description
R_m	1.68×10^{12}	1/m	Clean membrane resistance
θ	0.005	–	Fraction of SMP deposited on the membrane
k_{i0}	1.1×10^{16}	m/kg	SMP deposit resistance
α_0	4.0×10^{15}	m/kg	Cake resistance
$\triangle P_{\mathrm{crit}}$	30,000	Pa	Critical TMP below which compression does not occur
k_r	150	1/d	Cake removal rate constant
d_{crit}	0.005	Mm	Cake thickness above which sloughing starts to occur
k_{r1}	0.012	kg/m²/day	Cake detachment rate constant
k_{r2}	10.42	kg/m³/s	Cake detachment rate constant
$\mathrm{Flux}_{\mathrm{min}}$	30	l/(m² h)	Flux, below which no SMP deposition occurs
k_{SMP}	0.8	–	SMP deposition vs. flux dependency
γ_m	0.1	1/(Pa day)	Constant
τ_m	1000	Pa	Shear stress
λ_m	0.01	–	Static friction coefficient
γ_{flux}	0.002	1/s	Wall shear rate
n_{flux}	1.5	–	Exponent in back-transport model
k_{flux}	0.07	$m/(s^{1-n})$	Proportionality coefficient for back-transport

3.3. Calibration results – long-term filtration experiment

Reversible and irreversible fouling processes occur at very different time-scales. Reversible fouling can happen very quickly in a range of seconds to minutes and its impact can be reduced or completely eliminated with backwashing, air-scouring or provision of cross-flow velocities. The irreversible fouling in turn is a long term process attributing to a slow but constant build-up of resistance in the membrane. The reason behind calibrating the model on long term 650 hour long data was to test the flux dependent SMP submodel as the flux stepping experiment offered only a 5 hour set of information where irreversible fouling had only a very limited contribution to the build up of total membrane resistance. The model used in this calibration exercise was the basic model (Option 1) with flux dependent SMP deposition rate. Due to very high cross-flow

velocities in the pilot plant and the lack of information about cross-flow rates, cake detachment process has been modelled with the $k_r \cdot m_r$ term as in the original Liang formulation.

In order to fit the output of the model to measurements, the data had to be split into 5 sections (see Fig. 5). For each of these data sets the model has been calibrated individually. Two parameters have been used for calibration: cake detachment rate (k_r) and SMP deposition fraction (f_{SMP}). Values of the calibrated parameters for each calibration period are shown in Table 5. Clean membrane resistance (R_m) has been set to 16.5E+11 m⁻¹. For critical flux a value of 19 l/m²/h was used. Other model parameter values were carried forward from the first calibration exercise.

For visualisation purposes the model output was filtered to isolate forward filtration data from back-wash periods. Then, the 2-second measurements of

Table 4
Pilot MBR plant operational data

| *MBR plant (with bioreactor)*	
Membrane type and area	Vertical ''Puron'' fibres; PES 0.04 μm pore size; 20 m²
Permeate flow; backwash flow	0.6 m³/h; 1.1 m³/h
Permeate recirculation flow	0.27 m³/h
Backwash interval and duration	Every 6 min with 45 s ON
TMP	300–500 mbar
Bioreactor DO operating range	2–4 mg/L
Full air scour flow	27 Nm³/h for 15 s every 60 s
Low air scour flow	∼2 Nm³/h for 45 s every 60 s
Bioreactor data (membrane feed)	MLSS concentration ∼ 7500 mg/L
Bioreactor tank data	Volume 1 m³; operating level of weir 1.9–2.0 m
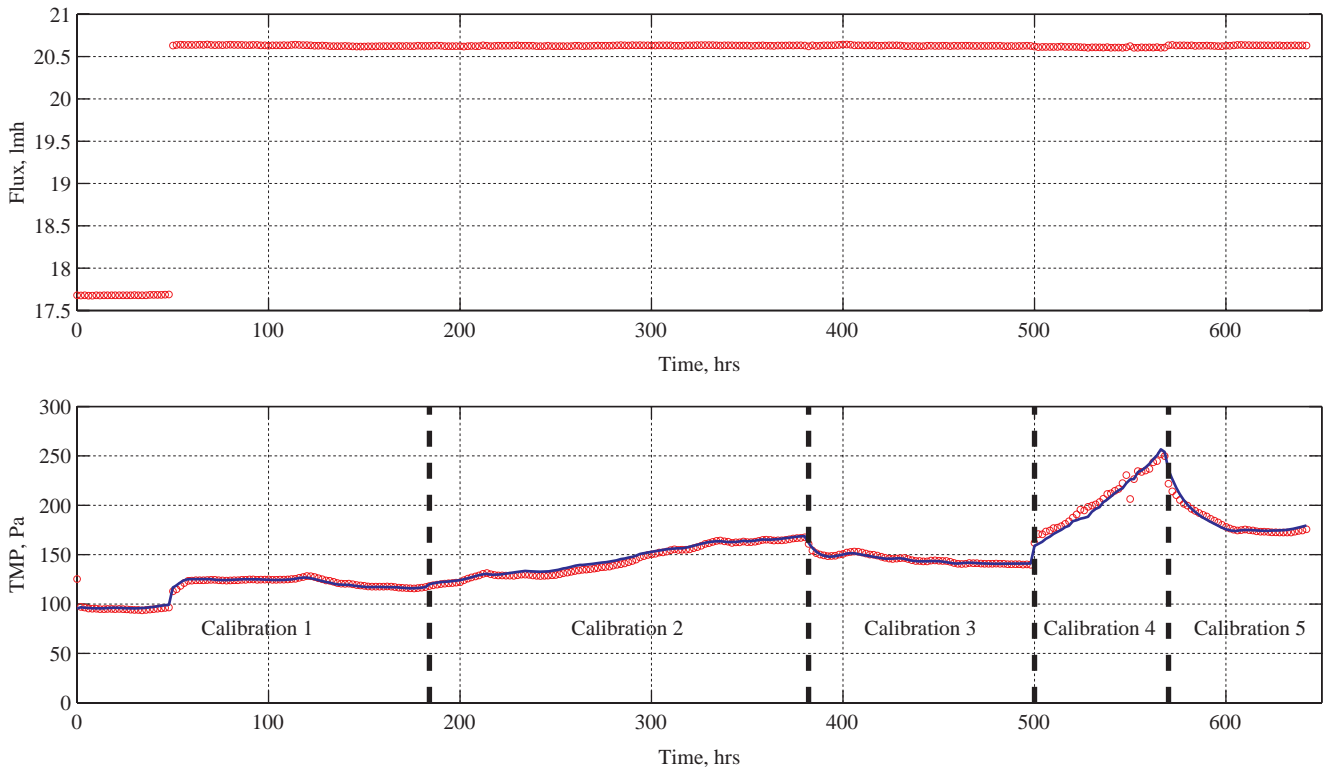
Fig. 5. Excerpt from long-term filtration experiment, 13 h:53 min–16 h:38 min.

both the flux and pressure have been averaged to obtain 2-hour averages. Flux (input to the model) and the measured and simulated TMPs are shown in Fig. 5. As the figure indicates, the model performed very well at predicting TMP for each and every calibration period.

In calibration sets 3 and 5, the TMP was found to decrease in time with flux remaining constant which indicated a gradual increase in membrane s permeability. The reason for this was unknown and due to very little information about operational conditions at this pilot-plant we assumed that the increase of permeability might be due to chemical forward flush or redissolution of the irreversible foulant from the membrane surface and pores. The observed increase in permeability has been modelled with exponential decay of the mass of irreversible foulant (m_i) as shown in Fig. 6. The measured flux and the measured and simulated TMPs for the calibration period 3 are shown in Fig. 7.

The model and experimental TMPs have been found to diverge slightly in backwash cycles (not shown). This difference is probably due to several reasons. Firstly the backwashing submodel is very crude and instantaneously removes all cake built up during forward filtration which does not happen in reality.

Also since the backwash flow is almost double the forward flow but only lasts a fraction of the time, pressure transients developing during instantaneous changes in the direction of flow would have caused fluctuations of pressure and flow which cannot be represented by the filtration model.

4. Conclusion

The Liang's model in its original form was able to pick up some general trends in the filtration process, but was lacking accuracy under some operating conditions as shown in the short term calibration exercise. The model was therefore expanded with several mathematical formulas which improved its predictability in terms

Table 5
Parameters calibrated in the long-term calibration experiment

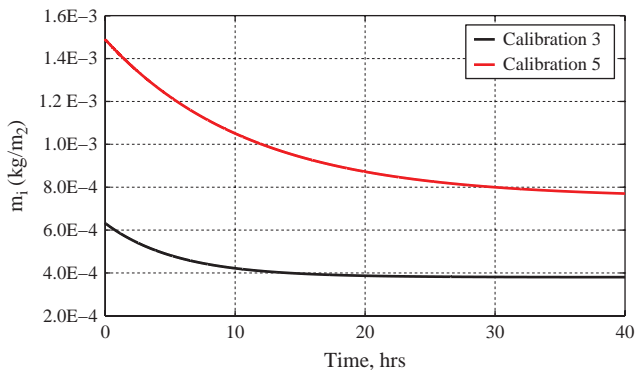|	k_r, d^{-1}	f_{SMP}, -
Calibration 1	0.75E+04	0.0008
Calibration 2	0.35E+04	0.0010
Calibration 3	0.85E+04	0
Calibration 4	0	0.0250
Calibration 5	0.85E+04	0

Fig. 6. Exponential decay of m_i in time during the calibration periods 3 and 5.

of both reversible and irreversible fouling. Major add ons were: flux dependent SMP deposition, cake thickness dependent cake removal, shear stress model relating cake detachment to air flow rates and cross flow velocities and Ho and Zydney's back transport model [21]. Computed TMPs from the modified model were in a good agreement with experimental data in both the flux stepping experiment and the long-term subcritical filtration experiment. This provided a reasonable proof that the model is able to predict TMPs during membrane ultrafiltration.

To make this proposed model more comprehensive additional research and investigation is needed in the following areas:

1. Development of a connection between the bound EPS concentration in the mixed liquor and the specific resistance of sludge cake, α.
2. Correlation of the cake detachment rate constant, k_r with crossflow velocity and/or air flow rates for sparging for various MBR configurations.
3. Modelling of an increase in cake adhesion to membrane surface with progressing irreversible fouling due to higher velocity fields around smaller (constricted) diameter pores.
4. Creation of a mechanistic backwash model which will be a function of backwash intensity, cake properties, shear stress, or similar parameters affecting the rate of cake removal. One such model has been presented in the work of Gehlert et al. [24] where cake removal is modelled by Eq. (17).

$$\left.\frac{dm_c}{dt}\right|_{\text{back}} = J \cdot X_{T,\text{back}} - \gamma_{\text{back}} \cdot (\tau - \lambda \cdot \text{TMP}) \cdot m_c \qquad (17)$$

Pressure loss during backwash is calculated in a similar way as for standard filtration but a
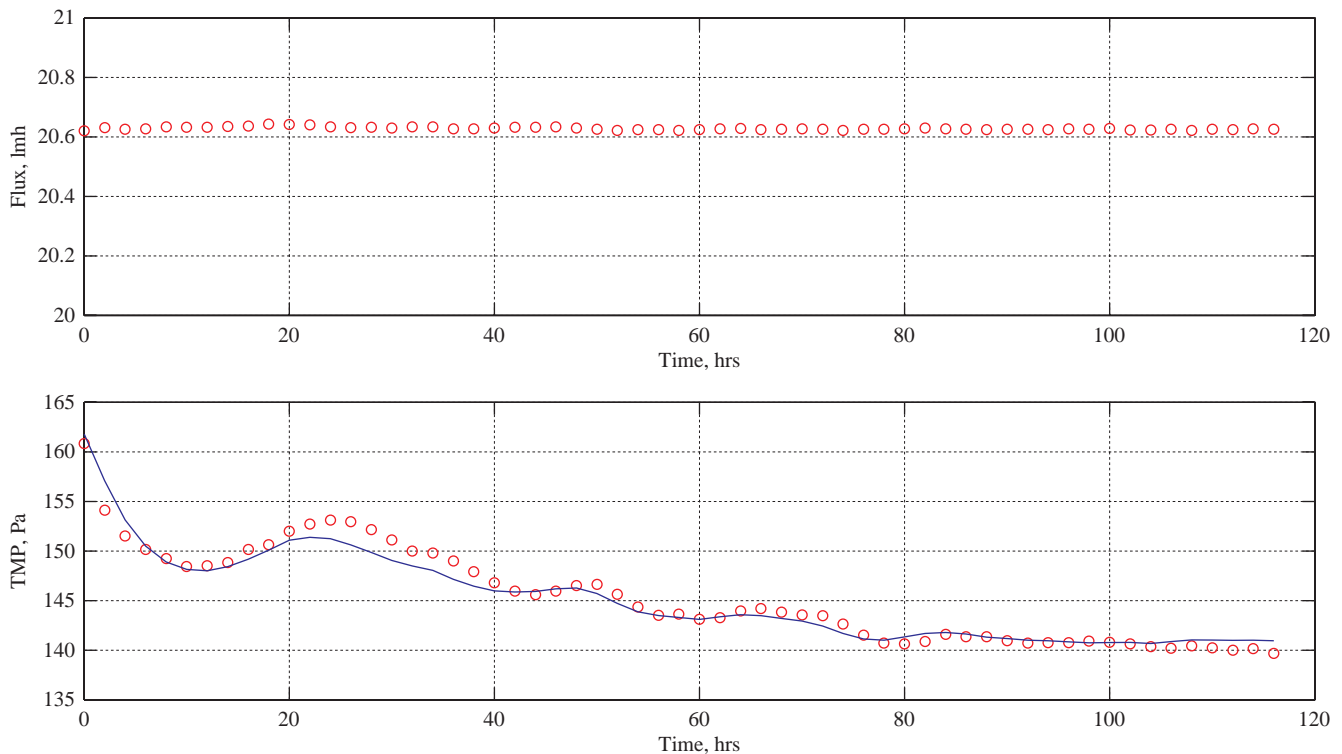

Fig. 7. Results of model calibration during the calibration period 3.

different specific cake resistance, α as shown in Eqs. (18) and (19).

$$\alpha = \alpha_{\text{back}} \tag{18}$$

$$R_{c,\text{back}} = \alpha_{\text{back}} \cdot m_c \tag{19}$$

Acknowledgments

References

[1] G. Tchobanoglous, F.L. Burton and H.D. Stensel, Wastewater Engineering, Treatment and Reuse, McGraw-Hill Professional, 2003, ISBN 0070418780, 9780070418783.
[2] S. Liang, L. Song, G. Tao, K.A. Kekre and H. Seah, A modelling study of fouling development in membrane bioreactors for wastewater treatment, Water Environ. Res., 78(8) (2006) 857-863.
[3] I.S. Chang, P. Le Clech, B. Jefferson and S. Judd, Membrane fouling in membrane bioreactors for wastewater treatment, J. Environ. Eng., 128(11) (2002) 1018-1029.
[4] C. Wisniewski and A. Grasmick, Floc size distribution in a membrane bioreactor and consequences for membrane fouling, Colloids Surf. A Physicochem. Eng. Aspects, 138 (1998) 403-411.
[5] F. Meng and F. Yang, Fouling mechanisms of deflocculated sludge, normal sludge, and bulking sludge in membrane bioreactor, J. Membr. Sci., 305 (2007) 48-56.
[6] H. Choi, K. Zhang, D.D. Dionysiou, D.B. Oerther and G.A. Sorial, Effect of permeate flux and tangential flow on membrane fouling for wastewater treatment, Sep. Purif. Technol., 45 (2005) 68-78.
[7] P.H. Nielsen and A. Jahn, in: J. Wingender, T.R. Neu, H.C. Flemming (Eds.), Microbial Extracellular Polymeric Substances, Springer, Berlin, 1999, pp. 49-72.
[8] C. Nuenghamnong, J.H. Kweon, J. Cho, C. Polprasert and K.H. Anh, Membrane fouling caused by extracellular polymeric substances during microfiltration processes, Desalination, 179 (2005) 117-124.
[9] P.H. Nielsen, A. Jahn and R. Palmgren, Conceptual model for production and composition of exopolymers in biofilms, Wat. Sci. Tech. 36 (1997) 11-19.
[10] K.M. Hsieh, G.A. Murgel, L.W. Lion and M.L. Shuler, Interactions of microbial biofilms with toxic trace metals: 1. Observation and modeling of cell growth, attachment, and production of extracellular polymer., Biotech. Bioeng. 44 (1994) 219-231.
[11] A. Broeckmann, J. Busch, T. Wintgens and W. Marquardt, Modeling of pore blocking and cake layer formation in membrane filtration for wastewater treatment, Desalination, 189 (2006) 97-109.
[12] P. Grelier, S. Rosenberger and A. Tazi-Pain, Influence of sludge retention time on membrane bioreactor hydraulic performance, Desalination, 192(1-3) (2006) 10-17.
[13] P.T. Hoa, L. Nair and C. Visvanathan, The effect of nutrients on extracellular polymeric substance production and its influence on sludge properties, Water SA, 29(Part 4) (2003) 437-442.
[14] C. Psoch and S. Schiewer, Resistance analysis for enhanced wastewater membrane filtration, J. Membr. Sci., 280 (2006) 284-297.
[15] H. Flemming, Biofouling bei Membranprozessen, Springer Verlag, Berlin, 1995, ISBN 3-540-58596-6.
[16] D. Lee and C. Wang, Review paper: theories of cake filtration and consolidation and implications to sludge dewatering, Water Res., 34(1) (2000) 1-20.
[17] K. Parameshwaran, A. Fane, B. Cho and K. Kim, Analysis of microfiltration performance with constant flux processing of secondary effluent, Water Res., 35(18) (2001) 4349-4358.
[18] Y. Ye, V. Chen and A.G. Fane, Modeling long-term subcritical filtration of model EPS solutions, Desalination, 191 (2006) 318-327.
[19] X.Y. Li and Y. Yuan, Collision frequencies of microbial aggregates with small particles by differential sedimentation, Environ. Sci. Technol., 36 (2002) 387-393.
[20] H. Nagaoka, S. Yamanishi and A. Miya, Modelling of biofouling by extracellular polymers in a membrane separation activated sludge system, Water Sci. Technol., 38(4-5) (1998) 497-504.
[21] C. Ho and A.L. Zydney, Overview of fouling phenomena and modelling approaches for membrane bioreactors, Sep. Sci. Technol., 41 (2006) 1231-1251.
[22] K. Shimizu, S. Takada, T. Takahashi and Y. Kawase, Phenomenological simulation model for gas hold-ups and volumetric mass transfer coefficients in external-loop airlift reactors, Chem. Eng. J., 84 (2001) 599-603.
[23] K. Krauth and K.F. Staab, Pressurized bioreactor with membrane filtration for waste-water treatment, Water Res., 27 (1993) 405-411.
[24] G. Gehlert, M. Abdulkadir, J. Fuhrmann and J. Hapke, Dynamic modeling of an ultrafiltration module for use in a membrane bioreactor, J. Membr. Sci., 248 (2005) 63-71.